

Research Article

Detection of Multicamera Pedestrian Trajectory Outliers in Geographic Scene

Wei Wang , Yujia Xie , and Xiaozhi Wang

Department of Information Engineering, Nanjing University of Finance & Economics, No. 3 Wenyuan Road, Nanjing, China

Correspondence should be addressed to Yujia Xie; 9120181003@nufe.edu.cn

Received 14 February 2022; Revised 7 March 2022; Accepted 18 March 2022; Published 13 April 2022

Academic Editor: Mohammad Farukh Hashmi

Copyright © 2022 Wei Wang et al. This is an open access article distributed under the Creative Commons Attribution License, which permits unrestricted use, distribution, and reproduction in any medium, provided the original work is properly cited.

The abnormal detection of moving objects in intelligent video surveillance system plays an important role in early warning for man-made disasters. However, the current abnormal detection methods cannot effectively perceive the cross-camera abnormal movements of video objects. The main reason is that the existing methods ignore the spatial relationship between the fields of view of different cameras and blind areas among the fields of view. This condition prevents them to effectively infer and analyze the cross-camera movements of video objects combined with geospatial information. This paper proposes the detection of multicamera pedestrian trajectory outliers in geographic scene to address this problem. This approach first spatializes the video object trajectory and then realizes trajectory vectorization by extracting trajectory points with equal time difference. The position trajectory outliers are detected by constructing isolation forest and scoring trajectory vectors, and the velocity trajectory outliers are identified through vectors' neighborhood comparison. Related experiments show that our method can effectively improve the efficiency and accuracy of detecting trajectory outliers, which can enhance the early warning capability of video surveillance systems for man-made disasters.

1. Introduction

In recent years, various man-made disasters have occurred frequently in human production and living places, causing immeasurable loss of lives and properties. Unlike natural disasters, the occurrence of man-made disasters often has early signs, and these signs are closely related to human abnormal behavior. We can provide early warning for disasters by detecting and analyzing abnormal behavior [1], which can be taken in advance to reduce or avoid the occurrence of man-made disasters. Human abnormal behavior is usually difficult to detect by using artificial methods. Thus, continuous monitoring and analysis of geographic scenes for detecting abnormal behavior are required. Intelligent video surveillance is an ideal approach for detecting human abnormal behavior. The identification and positioning of abnormal behavior can be realized by combining video and geographic information system (GIS). This process can provide efficient real-time technical support for early warning and emergency treatment of man-made disasters [2, 3].

With the development of surveillance video system from single camera to multicamera network [4], effective analysis of video data becomes challenging. In the field of abnormal detection, effectively determining whether abnormal behavior occurs on the basis of the motion of the video object in a single camera is often impossible. Comprehensively analyzing the video object's information in multiple cameras is necessary to reach an accurate conclusion. However, the current trajectory outlier detection methods can only analyze the object's trajectory in a single camera's field of view [5, 6]. These methods ignore the spatial relationship between the fields of view of different cameras and blind areas among the fields of view and cannot perceive the cross-camera abnormal movements of video objects. In response to the above problems, this paper proposes the detection of multicamera pedestrian trajectory outliers in geographic scene (Figure 1). Trajectory outliers are detected by analyzing the video object trajectories and the spatial elements of geographic scene. This approach first spatializes the video object trajectories by associating the trajectories of video objects in different cameras and then realizes trajectory vectorization

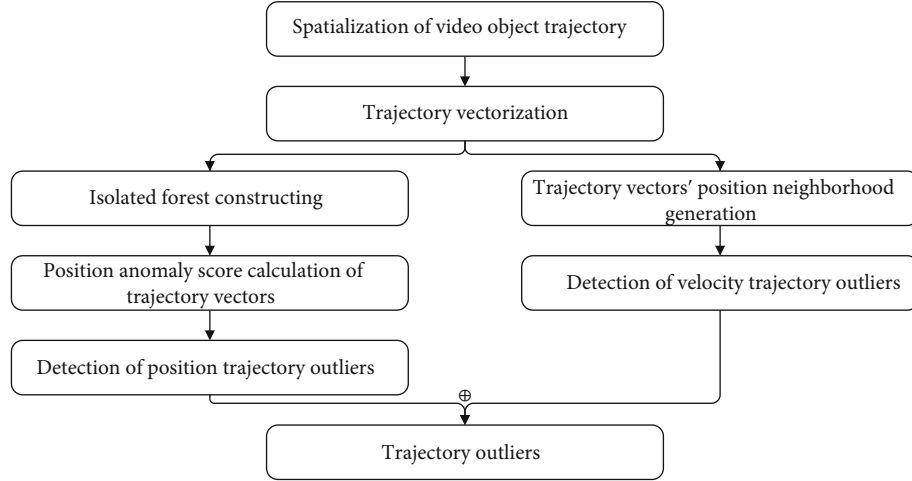


FIGURE 1: Flowchart of detection of trajectory outliers.

by extracting trajectory points with equal time difference. The position trajectory outliers are detected by constructing isolation forests and scoring trajectory vectors, and the velocity trajectory outliers are identified through vectors' neighborhood comparison. The types of trajectory outlier detection are divided into predefined outlier detection and undefined outlier detection [7]. The former determines whether the video object meets specific motion conditions to determine the anomaly, and the latter detects a small number of objects where their movement modes are different from a large number of video objects. This article only detects the undefined anomaly. This paper only detects outliers for pedestrian trajectories due to the large differences in the activity characteristics and the outlier determination criteria between pedestrians and vehicles [8].

The rest of this paper is organized as follows: Section 2 introduces the related research work. Section 3 describes the methods of spatialization and vectorization of video object trajectories in geographic scene. Section 4 presents the detection method of position trajectory outliers. Section 5 presents the detection of velocity trajectory outliers. Section 6 analyzes the related performance of this method through experiments. Finally, Section 7 provides the conclusion and summary of this paper.

2. Related Works

This paper involves three research fields: Video+GIS disaster management, video-geographic scene data fusion organization, and video object trajectory outlier detection. The related researches are as follows.

2.1. Video+GIS Disaster Management. For the research of video combined with GIS in the field of disaster management, the causes of disasters are classified into natural disasters, such as fire [9], extreme weather [10], and man-made disasters [11]. The response areas are divided into disaster early warning and preparedness and disaster emergency response. Research on disaster prevention is mainly used for early warning of abnormal crowd behavior associated

with man-made disasters, such as crowd abnormal motion detection [12] and scene population statistics [13]. In disaster emergency response, relevant research mainly integrates the video transmitted by unmanned aerial vehicle [14, 15], balloon [16], satellite [17], and other platform load cameras with GIS information to evaluate and analyze the disaster situation. For specific research, one mainly focuses on the system construction level, and the other mainly focuses on the data analysis level. The former includes as CCTV-based disaster identification and response system [18], adaptive emergency video communication system [19], and cloud computing perception analysis system [20]. The latter includes disaster loss assessment using spatial video [3], disaster semantic integration based on text report and on-site video [21], and disaster video detection based on deep learning [22].

2.2. Video-Geographic Scene Data Fusion Organization. The data fusion organization of video and geographic scene is the basis of video target analysis combined with geospatial information. On the basis of the concepts of multimedia GIS [23], geo-video [24], and video GIS [25], previous research constructed data organization methods, such as metadata description method [26] and global positioning system association method [27], and realized the geographic retrieval and playback of video images by describing the geographic location of video frames.

In recent years, more attention has been paid to the fusion of video content and geographical scene. A video scene data fusion organization method has been formed on the basis of camera spatial model [28] by constructing the image-geospatial mapping relationship [29]. Typical camera spatial models include quadrilateral model in 2D scene [30] and pyramid model in 3D scene [31]. On the basis of the developed data fusion organization methods of the above model, such as R-tree index based on view [32] and camera topological relationship [33], the data are fused and organized by analyzing the spatial relationship of cameras' fields of view. The other method uses texture association [34], spatiotemporal behavior association [35], semantic association

[36], and other methods of moving target to fuse and organize data.

2.3. Detection of Video Object Trajectory Outliers. The detection of video object trajectory outliers usually detects and extracts a small number of trajectories where their location or velocity is greatly different from other trajectories [37]. The common method is to detect trajectory outliers in unlabeled datasets by marking datasets [38, 39].

However, in practical application, labeled datasets are not always available due to the problems of complex trajectory shape and difficult real-time update of classifier; thus, some trajectory outlier detection methods use unlabeled datasets [40, 41]. Unlabeled dataset outlier detection is more efficient and accurate than labeled dataset outlier detection, but trajectory features are difficult to define accurately. At the algorithm level, trajectory outlier detection methods are mainly divided into two categories: distance-based and clustering-based methods. On the basis of the distance method, the differences in different attributes of trajectories are calculated, and then, the weighted sum of different differences is used to detect trajectory outliers. Typical methods include trajectory start and end+velocity direction detection method [42], t-partition detection method using minimum description length principle [1], and angle threshold division detection method [4]. However, such methods usually need accurate trajectory division, and time complexity is high. The trajectory dataset is reasonably clustered on the basis of clustering methods, and then, the detection of outliers is conducted. Typical methods include trajectory outlier detection methods based on neighborhood [43], feature learning model detection methods based on sparse coding [44], and anomalous point detection methods [45]. Although these methods use machine learning to improve the accuracy of trajectory outlier detection, they cannot be applied to unmarked trajectory datasets.

3. Vectorization of Video Object Trajectories in Geographic Scene

The video object trajectories in image space need to be transformed into geospatial trajectory vectors to realize the anomaly detection of video target in geographical scene. This chapter introduces related works of vectorization.

3.1. Spatialization of Video Object Trajectories. Trajectory spatialization needs to be realized first to realize trajectory vectorization. In this paper, video target subgraph and ground contact points are taken as positioning points sampled at a certain time interval [46]. The contact point of the video target with the ground will be transformed from image space into object space. The video object trajectories in the geographic scene are obtained by constructing the mapping relationship between image space and geospatial [28, 47], as shown in Figure 2.

In this paper, the mapping model is constructed by using projection matrix method. Assuming that q is the image coordinate of a point and Q is the geospatial coordinate, the homogeneous coordinates of q and Q can be expressed

as follows:

$$\begin{aligned} q &= [xy1]^T, \\ Q &= [XYZ1]^T. \end{aligned} \quad (1)$$

The projection matrix is calculated from the premeasured image space and geographic space corresponding to the same name point group data. Let the projection matrix be M , and the relationship between q and Q is as follows:

$$q = PQ. \quad (2)$$

After scaling, translation, and rotation transformation from image plane to the cameras' fields of view plane in geospatial, the projection matrix P can be decomposed into the following:

$$P = s \bullet W \bullet R, \quad (3)$$

where s is the scaling factor; W is the camera translation transformation matrix; R is the 3×4 D rotation transformation matrix.

$$\begin{aligned} W &= \begin{bmatrix} f_u & 0 & u \\ 0 & f_v & v \\ 0 & 0 & 1 \end{bmatrix}, \\ R &= [r_1 r_2 r_3 e], \end{aligned} \quad (4)$$

where f_u and f_v represent the product of the physical focal length of the lens and the size of the sensor in the transverse and longitudinal axes of each unit; u and v represent the offset of the image imaging center relative to the main optical axis in the horizontal axis and the vertical axis, respectively; r_1 , r_2 , and r_3 represent the rotation relationship of the coordinate system in the direction of X axis, Y axis, and Z axis in physical space, respectively; e represents the translation relationship between coordinate systems.

When using the projection matrix method, the cameras' fields of view plane in geospatial space are assumed to be a horizontal plane; that is, the plane is $Z = 0$. Therefore, the mapping relationship from image space to geospatial space can be regarded as the mapping from one plane to another. To simplify the calculation, we remove Z in Q and rotate r_3 around the Z axis in R . The projection matrix P is simplified as follows:

$$P = s \bullet \begin{bmatrix} f_u & 0 & u \\ 0 & f_v & v \\ 0 & 0 & 1 \end{bmatrix} \bullet [r_1 r_2 r_3 e]. \quad (5)$$

In accordance with the solution of matrix P , the geospatial coordinates of video object trajectories can be obtained.

3.2. Trajectory Vectorization. After spatialization in Section 3.1, map the positions of all video objects in each frame of surveillance videos to a unified 2D plane coordinate system

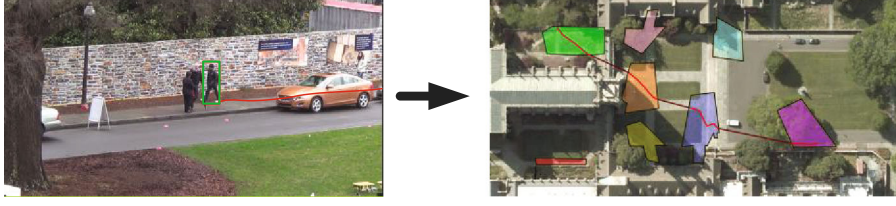


FIGURE 2: Schematic of the video object trajectory spatialization.

[46]. Through video image target reidentification, cross-camera trajectories' association can be achieved [48].

This paper presents a trajectory vectorization method based on position and azimuth. The video object trajectory Tra_i is represented as a set of 2D points.

$$Tra_i = \{p_{i,j} (j = 1, \dots, \text{len}_i)\}, \quad (6)$$

$$p_{i,j} = (x_{i,j}, y_{i,j}).$$

For $\forall Tra_i$, a set of trajectory vectors \neg is obtained through trajectory vectorization.

$$\neg_i = \{u_{i,k} (k = 1, \dots, \text{len}(Tra_i) - 1)\}, \quad (7)$$

$$u_{i,k} = [x_{i,k}, y_{i,k}, x_{i,k+1}, y_{i,k+1}, \theta_{i,k}]^T,$$

where θ represents the azimuth of the vector. The direction of 0° (usually chooses the north of the geographical position) is defined in the scene. For $\forall k$, the azimuth θ is defined as 0° rotates counterclockwise to the angle turned by $\overrightarrow{p_{i,k}, p_{i,k+1}}$.

The vectorization process of multicamera video object trajectories is shown in Figure 3. A trajectory (Tra_i) successively passes through 3 camera fields of view and 2 blind areas. For trajectories in cameras' fields of view, the position of adjacent frames is used as the starting points and end points of the vector. For trajectories in blind areas, the exit from the previous camera position and entry to the next camera position of trajectories are taken as starting points and end points of the vector.

4. Detection of Position Trajectory Outliers Based on Isolation Forest

Isolation forest [49], as a data anomaly detection method, is composed of a large number of isolation trees. Based on partition isolation and ensemble learning, the abnormal data is found by constructing a large number of isolation trees. For each isolation tree, a random hyperplane is designed to cut the data space. One cut can generate two subtrees and then continue to use a random cut until there is only 1 data point in each subtree. Due to the low density of abnormal data, the number of divisions is less than that of normal data, so the average depth is deeper on isolation forest. Isolation forest has the advantages of not needing to calculate related distance, density, and other indicators, low time complexity, and high recognition accuracy. Therefore, we use isolation forest to calcu-

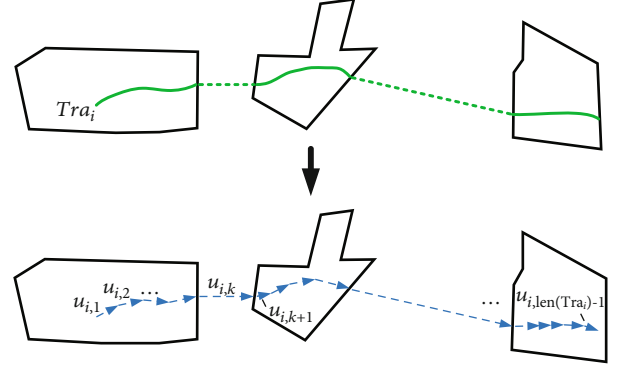


FIGURE 3: Schematic of multicamera trajectory vectorization.

late location anomaly score for trajectory vectors. The anomaly score for each trajectory vector is calculated by inputting all the trajectory vectors of the dataset into the isolation forest.

4.1. The Set of Trajectory Vector Generation. Each video target in the whole dataset is spatialized and vectorized, and then, all trajectory vectors are combined to obtain the set of trajectory vectors:

$$V = \bigcup \neg_i. \quad (8)$$

4.2. Isolation Tree Structure. The main steps to construct an isolation tree are as follows:

- (1) Randomly select s trajectory vectors from V as s root nodes of isolation trees (in this paper, $s = \lceil 1/60 \cdot N_T \rceil$, where N_T is the total trajectory vectors of T)
- (2) Randomly select one vector component
- (3) Randomly select a split value mid between the minimum and maximum values in the selected vector component. The split value divides the sample space into two subtrees, and the one less than mid is regarded as the left subtree. The one greater than mid is regarded as the right subtree
- (4) Repeat steps 2 and 3 for the two subtrees. Iterate continuously until only one trajectory vector is left on the leaf node or the depth of the specified tree is reached

Through the above steps, s isolation trees are constructed to form an isolation forest.

4.3. Position Anomaly Score Calculation of Trajectory Vectors. After Section 4.1, each trajectory vector u_i in each isolation tree is obtained. Since average depth of isolation trees grows in the order of $\log N_T$ [7], it has a structure equivalent to a BST [50]. We define the position anomaly score of the vector u_ϕ by the ratio of the depth expectation of u_ϕ to the average value of search path length in BST.

$$\text{Score}(u_\phi, p) = 2^{-E(h(u_\phi))/c(p)+1}, \quad (9)$$

where $h(u_k)$ is the depth of u_k in the isolation tree, $E(h(u_\phi))$ represents the depth expectation computed over all trees in the forest of u_ϕ , p represents the number of samples, and $c(p)$ represents the value of search path length in BST given the number of samples p [51].

$$c(p) = \begin{cases} 2H(p-1) - \frac{2(p-1)}{n}, & p > 2, \\ 1, & p = 2, \\ 0, & p < 2, \end{cases} \quad (10)$$

$$H(x) = \ln(x) + \xi,$$

where ξ represents the Euler constant. To consider the length difference between vectors in blind areas and vectors in camera's field of view, we make the following adjustment to obtain the anomaly score of vectors in blind areas. Assuming u_o is the vector in blind areas, its anomaly score (u_o, p) will be adjusted to the following:

$$\text{Score}'(u_o, p) = 2^{-E(h(u_o)) + \varepsilon/c(p)+1}, \quad (11)$$

$$\varepsilon = \frac{1/n_{\text{out}} \sum \|u_{\text{out}}\|}{1/n_{\text{in}} \sum \|u_{\text{in}}\|},$$

where $S_{I1}(\text{Tra}_i)$ and $S_{I2}(\text{Tra}_i)$ represent the proportion of trajectory position anomaly value and the number of trajec-

where ε represents the adjustment coefficient; n_{out} and n_{in} represent the number of vectors in blind areas contained in the trajectory of u_o and the number of vectors in camera's field of view contained in the trajectory of u_o ; u_{out} represents any vector in blind areas on the trajectory where u_o is located; u_{in} represents any vector in camera's field of view on the trajectory where u_o is located. $\|u_{\text{out}}\|$ and $\|u_{\text{in}}\|$ represent the norm of u_{out} and u_{in} , respectively.

The use of the depth expectation reflects the density of the nearby vector data, because the sparser the trajectory vector, the trajectory vector is easier to be separated in hyperplanes and the greater the possibility of abnormality [50]. The closer the value of $\text{score}(u_\phi, p)$ is to 1, the higher the probability that the sample is a trajectory outlier vector.

4.4. Detection of Position Trajectory Outliers. The traditional position trajectory outlier detection algorithm [1] regards the ratio of the number of abnormal segments to the total number of trajectory segments as the evaluation criteria. However, for the multicamera trajectory mentioned in this paper, sufficient abnormal segments may be ignored because the trajectory is extremely long. Therefore, we define the multicamera position trajectory outlier as a trajectory with a sufficient proportion of position trajectory outlier vectors or a sufficient number of position trajectory outlier vectors and evaluate it in terms of the trajectory position anomaly value. Determine whether $\forall \text{Tra}_i$ satisfies the following:

$$S_I(\text{Tra}_i) > T_I, \quad (T_I \in [0, 1]), \quad (12)$$

where Tra_i is a position trajectory outlier and T_I is the threshold of trajectory position outlier. The calculation method of $S_I(\text{Tra}_i)$ is as follows:

outlier vector number threshold (generally $\leq 1/2 \text{NUM}(u_{i,j} \in \text{Tra}_i)$). The closer μ_I is to 1 and the bigger is n_1 , the fewer

$$S_I(\text{Tra}_i) = \max(S_{I1}(\text{Tra}_i), S_{I2}(\text{Tra}_i)),$$

$$S_{I1}(\text{Tra}_i) = \frac{\text{NUM}(u_{i,j} \in \text{Tra}_i, (\text{score}(u_{i,j}, p) > \mu_I))}{\text{NUM}(u_{i,j} \in \text{Tra}_i)}, \quad (\mu_I \in [0, 1]),$$

$$S_{I2}(\text{Tra}_i) = \begin{cases} 1, & \text{NUM}(u_{i,j} \in \text{Tra}_i, (\text{score}(u_{i,j}, p) > \mu_I)) \geq n_1, \\ \frac{\text{NUM}(u_{i,j} \in \text{Tra}_i, (\text{score}(u_{i,j}, p) > \mu_I))}{n_1}, & \text{NUM}(u_{i,j} \in \text{Tra}_i, (\text{score}(u_{i,j}, p) > \mu_I)) < n_1 (n_1 \in N_+), \end{cases} \quad (13)$$

tory position anomaly value of trajectory Tra_i , NUM means counting, μ_I is the trajectory vector isolation forest score threshold (generally ≤ 0.5), and n_1 is the location trajectory

position trajectory outliers are detected. The specific value shall be set according to the actual demand and the experience of experts.

5. Detection of Velocity Trajectory Outliers Based on the Trajectory Vectors' Neighborhood

In this paper, the neighborhood comparison method is used to compare the velocity difference between adjacent trajectory vectors and determine the velocity trajectory outliers.

5.1. Trajectory Vectors' Position Neighborhood Generation. The concept of adjacency vectors for any trajectory vector is described as trajectory vectors within the circular position neighborhood. For $\forall u_\varphi = [x_\varphi, y_\varphi, x_{\varphi+1}, y_{\varphi+1}, \theta_\varphi]^T \in T$, if any trajectory vector $u_\lambda = [x_\lambda, y_\lambda, x_{\lambda+1}, y_{\lambda+1}, \theta_\lambda]^T \in T$ is the position neighborhood vector of u_φ , denoted as $\text{sim}_D(u_\varphi, u_\lambda)$, then u_φ, u_λ should satisfy the following:

$$\sqrt{(x_\varphi - x_\lambda)^2 + (y_\varphi - y_\lambda)^2} < D. \quad (14)$$

In particular, if u_φ is a vector in blind areas, in addition to satisfying Equation (14), it must also satisfy the following:

$$\sqrt{(x_{\varphi+1} - x_{\lambda+1})^2 + (y_{\varphi+1} - y_{\lambda+1})^2} < D. \quad (15)$$

Specifically, the neighborhood vectors of the trajectory vector in cameras' field of view are defined as trajectory vectors adjacent to the starting point. The neighborhood vector of the trajectory vector in blind areas is defined as trajectory vectors adjacent to the exit point of the previous camera and the entry point of the next camera. Figure 4 shows the neighborhood representation method of the trajectory vectors in different situations. The green arrow represents the original trajectory vector, the red circle represents the neighborhood of the beginning and end of the trajectory vector, and blue arrows represent the neighborhood vectors.

5.2. Detection of Velocity Trajectory Outliers. Due to different scenes, the average speed of pedestrians under each camera

is very different. We cannot simply use velocity threshold to detect anomalies in trajectories under different cameras. We define the multicamera velocity trajectory outlier as a trajectory with a sufficient proportion of velocity trajectory outlier vectors where the standard deviation of the neighborhood exceeds the threshold or a sufficient number of trajectory vectors where the standard deviation exceeds the threshold. Evaluation is made on the basis of trajectory velocity anomaly value.

On the basis of the result of the neighborhood generation of trajectory vectors, the velocity trajectory outliers are detected by comparing the velocity of the original vector with the vector in the neighborhood. The velocity of the trajectory vector is described as the norm of the trajectory vector to time.

$$v(u_\varphi) = \frac{\sqrt{(x_{\varphi+1} - x_\varphi)^2 + (y_{\varphi+1} - y_\varphi)^2}}{\Delta t}, \quad (16)$$

where Δt is the sampling time difference between the beginning and the end of the vector. We use the standard deviation of the velocity of the trajectory vector and its neighborhood vectors to judge velocity outliers. Given the trajectory vector $u_{i,j}$ in trajectory Tra_i , its standard deviation $\text{SD}(u_{i,j} \in \text{Tra}_i)$ is as follows:

$$\text{SD}(u_{i,j} \in \text{Tra}_i) = \sqrt{\frac{1}{\text{NUM}(\text{sim}_D(u_{i,j}, u_\varphi))} \sum_{\text{sim}_D(u_{i,j}, u_\varphi)} (v(u_{i,j}) - v(u_\varphi))^2}. \quad (17)$$

Determine whether $\forall \text{Tra}_i$ satisfies the following:

$$S_v(\text{Tra}_i) > T_v, \quad (T_v \in [0, 1]), \quad (18)$$

where Tra_i is a velocity trajectory outlier and T_v is the threshold of trajectory velocity anomaly. The calculation method of $S_v(\text{Tra}_i)$ is as follows:

$$\begin{aligned} S_v(\text{Tra}_i) &= \max(S_{v1}(\text{Tra}_i), S_{v2}(\text{Tra}_i)), \\ S_{v1}(\text{Tra}_i) &= \frac{\text{NUM}(\text{SD}(u_{i,j} \in \text{Tra}_i) > \mu_v)}{\text{NUM}(u_{i,j} \in \text{Tra}_i)}, \\ S_{v2}(\text{Tra}_i) &= \begin{cases} 1, & (\text{NUM}(\text{SD}(u_{i,j} \in \text{Tra}_i) > \mu_v)) \geq n_2, \\ \frac{\text{NUM}(\text{SD}(u_{i,j} \in \text{Tra}_i) > \mu_v)}{n_2}, & (\text{NUM}(\text{SD}(u_{i,j} \in \text{Tra}_i) > \mu_v)) < n_2, \end{cases} \end{aligned} \quad (19)$$

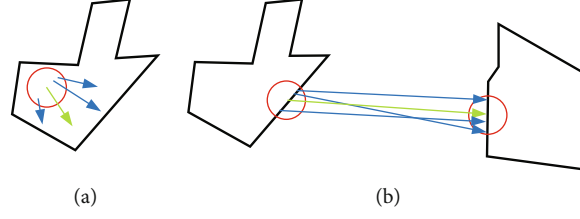


FIGURE 4: Schematic of trajectory vector neighborhood and neighborhood vectors. (a) Beginning point neighborhood of the trajectory vector and its neighborhood vectors in the single camera's field of view. (b) Beginning and end of the trajectory vector and its neighborhood vectors in camera blind areas.

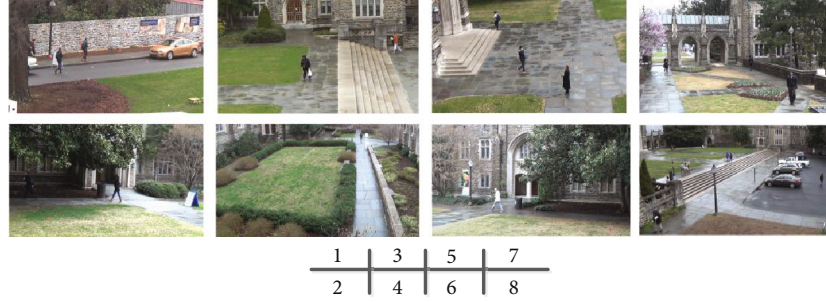


FIGURE 5: Eight channels of surveillance video image.

where $S_{v1}(\text{Tra}_i)$ and $S_{v2}(\text{Tra}_i)$ represent the proportion of velocity anomaly value and the number of trajectory velocity anomaly value of trajectory Tra_i , μ_v is the threshold of the mean of standard deviation, n_2 is the number of velocity trajectory outlier vectors' number threshold, and $n_2 \in N_+$, respectively. The parameter selection rules here are the same as for location trajectory outliers.

6. Experimental Analysis

6.1. Experimental Environment. The experimental data in this paper are the open-source data provided by DukeMTMC [46]. These data include 8 channels of video image data synchronously captured by cameras with fixed spatial position and attitude (Figure 5), and geographical position data of all cameras and cameras' field of view and camera correction parameters (Figure 6). The data also include more than 1845 cross-camera dynamic object trajectories that are marked by the image bounding box generated by automatic detection and tracking by computer vision +manual labeling and correction. In this experiment, all of trajectories in DukeMTMC are selected as the experimental data.

Experimental environment includes software (Windows 10, Python3.6+ sklearn0.0) and hardware (Intel(R) Core (TM) i7-10510U CPU @ 1.80 GHz, RAM 12.0 GB, NVIDIA GeForce MX250).

The preprocessing algorithm of obtaining video moving target trajectories is as follows: the video dynamic object detection algorithm is Mask-RCNN [52], the tracking algorithm is CSRT [53], and the cross-camera recognition algorithm is an improved method to generate unlabeled samples based on generative adversarial network [54].

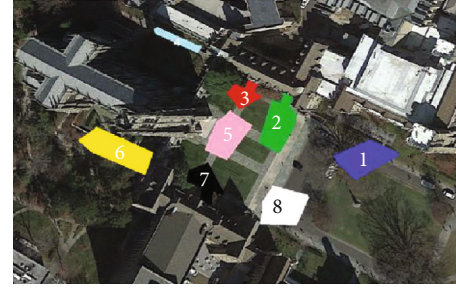


FIGURE 6: Camera's field of view distribution of monitoring camera.

6.2. Detection and Analysis of Position Trajectory Outliers. We choose trajectory outlier detection methods based on segmentation but based on distance and clustering for comparison. Results show that the method of this paper is more efficient than the traditional.

The original dataset lacks the true value of position trajectory outliers [55]. Taking each trajectory as a sample, we selected five volunteers for each sample to manually vote to determine the position trajectory outliers. At least two of the five volunteers' considered position trajectory outliers are taken as negative samples and other trajectories as positive samples (position normal trajectories). After the above manual processing, we extracted 316 negative samples from 1845 video target trajectories, with an exception rate of 17%.

To realize the effective selection of parameters, we use $F1$ -score [56] index to obtain the harmonic average of accuracy and recall through calculation for parameter optimization. When the maximum value $F1$ is taken, we substitute the corresponding parameters as the optimal parameters in the subsequent experiments.

TABLE 1: $F1$ value under different parameter value combinations.

(a)						
	$T_1 = 0.1$	$n_1 = 9$ $T_1 = 0.21$	$T_1 = 0.24$	$T_1 = 0.1$	$n_1 = 18$ $T_1 = 0.21$	$T_1 = 0.24$
$\mu_1 = 0.1$	0.901	0.878	0.569	0.901	0.891	0.633
$\mu_1 = 0.3$	0.900	0.900	0.668	0.900	0.935	0.797
$\mu_1 = 0.5$	0.900	0.896	0.669	0.899	0.931	0.806
$\mu_1 = 0.9$	0.899	0.894	0.668	0.899	0.928	0.802

(b)						
	$T_1 = 0.1$	$n_1 = 24$ $T_1 = 0.21$	$T_1 = 0.24$	$T_1 = 0.1$	$n_1 = 30$ $T_1 = 0.21$	$T_1 = 0.24$
$\mu_1 = 0.1$	0.901	0.891	0.635	0.901	0.892	0.636
$\mu_1 = 0.3$	0.900	0.944	0.857	0.900	0.938	0.883
$\mu_1 = 0.5$	0.899	0.939	0.872	0.899	0.932	0.905
$\mu_1 = 0.9$	0.899	0.936	0.868	0.899	0.929	0.900

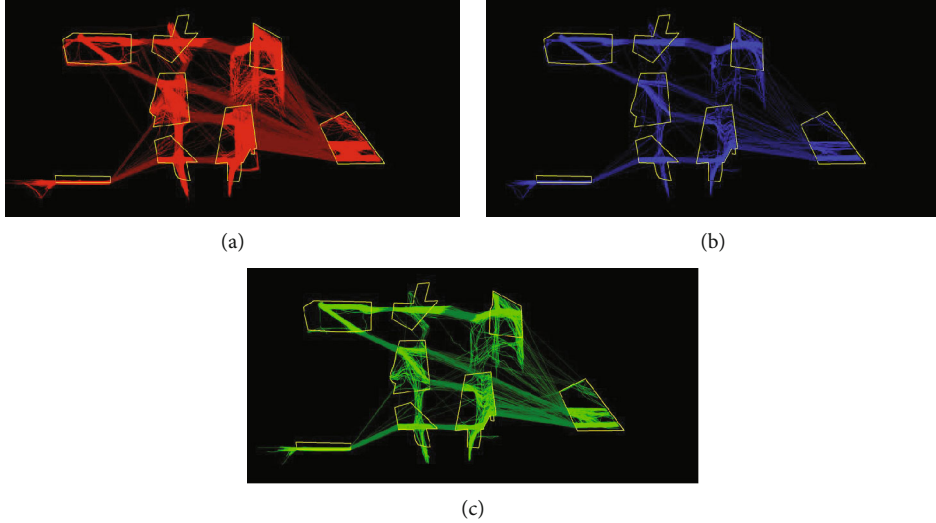


FIGURE 7: Detection results of undefined position trajectory outliers: (a) DukeMTMC dataset trajectories; (b) manually marked trajectory outliers; (c) trajectory outliers detected by position trajectory outlier detection method.

$$F1 = \frac{2 \cdot \text{precision} \cdot \text{recall}}{\text{precision} + \text{recall}}. \quad (20)$$

In accordance with the above formula, calculate the value of $F1$ under different parameter value combinations, as shown in Table 1.

As shown in Table 1, when the parameter is $n_1 = 24$, $T_1 = 0.21$, $\mu_1 = 0.3$, the maximum value is $F1$. We take this group of parameters for the detection of trajectory outliers, and the results are shown in Figure 7.

We use density-based segmentation detection method [57] and distance-based segmentation detection method [1] to compare and verify the effectiveness of our method.

Like this paper, we optimized other method parameters and use a receiver operating characteristic-area under the curve (ROC-AUC) evaluation system [58] to compare and analyze the detection effects of these methods in the best case. ROC curve is a graph with false positive rate (FPR) as the horizontal axis and true positive rate (TPR) as the vertical axis. AUC represents the area enclosed by ROC curve and its coordinate axis.

$$AUC = \frac{1}{2} \sum_{i=1}^{m-1} (FPR_{i+1} - FPR_i) \cdot (TPR_{i+1} - TPR_i), \quad (21)$$

$$FPR = \frac{FP}{FP + TN},$$

$$TPR = \frac{TP}{TP + TN},$$

TABLE 2: Contingency table.

	Estimate	True	False
	Truth value		
True		TP	FN
False		FP	TN

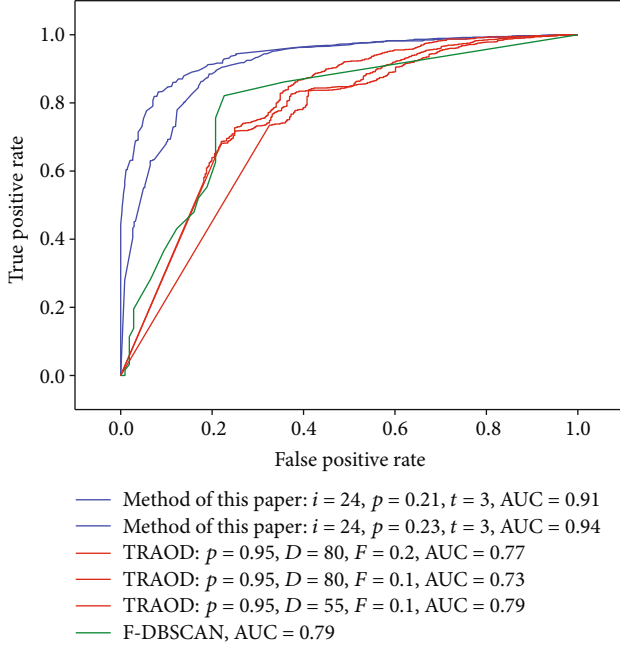


FIGURE 8: RAC curves and AUC values of our method, TRAOD, and F-DBSCAN in the best case.

TABLE 3: Processing time of different algorithms on the DukeMTMC dataset.

Method	Our method	TRAOD	F-DBSCAN
CPU time	124.06 s	14864.30 s	36255.07 s

where the definitions of TP, TN, FN, and FP are shown in Table 2.

As shown in Figure 8, we take some groups of parameters for each method and draw the ROC curves of three algorithms. The maximum AUC value of the proposed method is 0.94, which is higher than that of the two traditional methods by 0.79, indicating that the proposed method has lower false detection rate and higher recall rate compared with the two other methods. Through the analysis of the principle of the algorithm, we believe that the traditional clustering-based detection method cannot well determine the cluster center, and the distance-based detection method cannot accurately define the distance between trajectory segments, especially the angular distance between trajectories. The two traditional methods only consider the proportion of abnormal segments in the whole trajectory. Generally, for multicamera trajectories, position anomalies account for a small proportion. Thus, these methods cannot correctly detect trajectory outliers. The definition of position trajec-

TABLE 4: Number of velocity trajectory outliers under the combination of different parameters.

(a)						
	$n_2 = 5$			$n_2 = 10$		
	$T_v = 5$	$T_v = 10$	$T_v = 20$	$T_v = 5$	$T_v = 10$	$T_v = 20$
$\mu_v = 1.15$	779	754	752	660	463	424
$\mu_v = 1.4$	497	476	475	390	201	173
$\mu_v = 1.65$	221	204	202	152	52	36
$\mu_v = 1.9$	94	82	79	75	27	17

(b)						
	$n_2 = 15$			$n_2 = 20$		
	$T_v = 5$	$T_v = 10$	$T_v = 20$	$T_v = 5$	$T_v = 10$	$T_v = 20$
$\mu_v = 1.15$	657	349	206	656	346	158
$\mu_v = 1.4$	387	160	94	386	153	78
$\mu_v = 1.65$	151	45	14	151	45	13
$\mu_v = 1.9$	75	24	8	75	24	7

tory outliers in this paper considers the proportion and number of trajectory vectors, thereby overcoming the shortcomings of traditional methods.

We investigate the time efficiency of the algorithm. The processing time of the algorithm is counted in accordance with the parameters when the highest AUC value is taken for each algorithm. The results are shown in Table 3.

As shown in Table 3, the processing time of the proposed algorithm is 124.06 s. The processing times of TRAOD and F-DBSCAN are 14864.30 and 36255.07 s, respectively. The results show that the efficiency of the proposed algorithm is better than that of the traditional method when the datasets are the same.

6.3. Detection and Analysis of Velocity Trajectory Outliers. In practice, different scenarios or different users' intentions will lead to different velocity trajectory outliers. We select different threshold values of standard deviation μ_v for algorithm analysis. We detect multicamera velocity trajectory outliers by setting different parameters in $D = 5$ m, and the number of trajectory outliers detected under each parameter is shown in Table 4.

We show the velocity trajectory outliers under the four parameters of $n_2 = 10, \mu_v = 1.65, T_v = 20$, $n_2 = 10, \mu_v = 1.65, T_v = 5$, $n_2 = 10, \mu_v = 1.9, T_v = 20$, and $n_2 = 20, \mu_v = 1.65, T_v = 20$, as shown in Figure 9. All of the trajectories not shown in Figure 9 are normal velocity trajectories. Green segments indicate the part with normal velocity, and red segments represent the part with abnormal velocity.

Figure 9(a) shows the result of outlier detection of $n_2 = 10, \mu_v = 1.65, T_v = 20$, and Figure 9(b) shows the result of outlier detection of $n_2 = 10, \mu_v = 1.65, T_v = 5$, where n_2 and μ_v are unchanged compared with Figure 9(a). Trajectory outliers in Figure 9(a) are a subset of trajectory outliers in

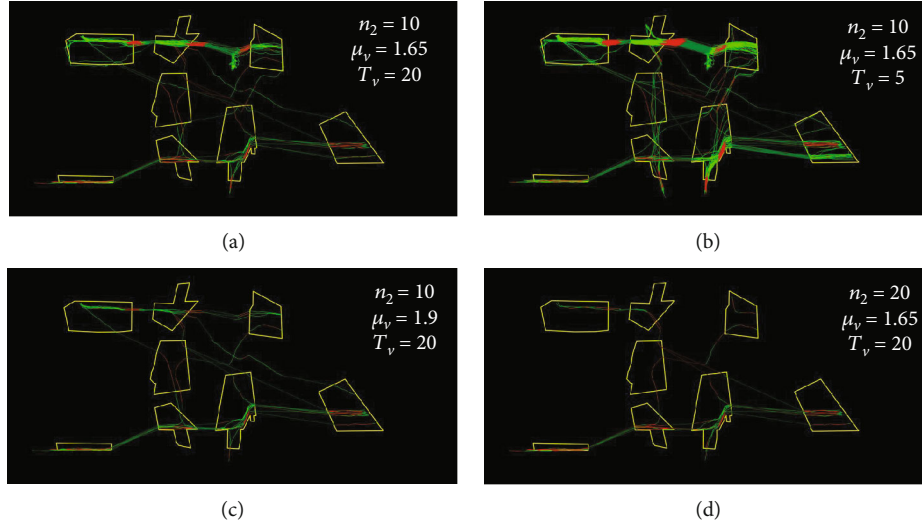


FIGURE 9: Schematic of multicamera velocity trajectory outliers: (a) the result of velocity trajectory outlier detection of $n_2 = 10$, $\mu_v = 1.65$, $T_v = 20$; (b) the result of velocity trajectory outlier detection of $n_2 = 10$, $\mu_v = 1.65$, $T_v = 5$; (c) the result of velocity trajectory outlier detection of $n_2 = 10$, $\mu_v = 1.9$, $T_v = 20$; (d) the result of velocity trajectory outlier detection of $n_2 = 20$, $\mu_v = 1.65$, $T_v = 20$.

Figure 9(b). Figure 9(c) shows the result of outlier detection of $n_2 = 10$, $\mu_v = 1.9$, $T_v = 20$. Compared with Figure 9(a), no change is observed in n_2 and T_v but μ_v increases. Thus, some abnormal segments in Figure 9(a) are no longer detected as outliers in Figure 9(c), resulting in a decrease in the number of trajectory outliers. Compared with Figure 9(a), Figure 9(d) shows the result of trajectory outlier detection of $n_2 = 20$, $\mu_v = 1.65$, $T_v = 20$. Compared with Figure 9(a), μ_v and T_v are unchanged but n_2 increases. Therefore, some trajectory outliers in Figure 9(a) are no longer detected as outliers because they cannot reach the new threshold of the number of abnormal segments, resulting in a decrease in the number of trajectory outliers. Trajectory outliers in Figure 9(d) are a subset of trajectory outliers in Figure 9(a).

The proposed method can get different outlier detection results by adjusting the relevant parameters to relax or tighten the standard.

7. Conclusions

This paper proposes a multicamera pedestrian trajectory outlier detection method in geographical scene to solve the problem that the current trajectory outlier detection methods cannot effectively infer and analyze the cross-camera abnormal movements of video objects based on geospatial information. The proposed method is based on the spatialization and vectorization of video object trajectories. Position trajectory outliers are detected by the isolation forest, and velocity trajectory outliers are detected through vectors' neighborhood comparison. The experimental results show that the recall, precision, and efficiency of this method are higher than those of the traditional algorithm. In this method, different velocity trajectory outlier detection results can be obtained by adjusting the relevant parameters to relax or tighten the detection standards. This paper does not combine the spatial semantic features of geographical scenes for trajectory anomaly analysis. Therefore, in the future work,

we will study a more scene adaptive video target anomaly detection method.

Data Availability

The data used to support the findings of this study are included within the article.

Conflicts of Interest

The authors declare that they have no conflicts of interest.

Authors' Contributions

Conceptualization was supervised by Wei Wang. Methodology was supervised by Wei Wang. Software was supervised by Wei Wang. Validation was supervised by Wei Wang. Formal analysis was supervised by Wei Wang. Investigation was supervised by Wei Wang. Resources were supervised by Wei Wang. Data curation was supervised by Wei Wang. Writing the original draft preparation was supervised by Wei Wang and Yujia Xie. Writing the review and editing was supervised by Wei Wang, Yujia Xie, and Xiaozhi Wang. Visualization was supervised by Wei Wang. Supervision was headed by Wei Wang. Project administration was supervised by Wei Wang. Funding acquisition was supervised by Wei Wang.

Acknowledgments

This research was funded by the National Natural Science Foundation of China (NSFC) under (Grant no. 41801305), the Open Research Fund of State Key Laboratory of Surveying, Mapping and Remote Sensing Information Engineering, Wuhan University, under (Grant no. 21S03), and the Research on Video-Geographic Scene Fusion Expression Based on Eye Movement Data, Nanjing University of Finance & Economics (Grant no. KYCX20-1323).

References

- [1] J. G. Lee and J. Han, "Trajectory outlier detection: a partition-and-detect framework," in *2008 IEEE 24th International Conference on Data Engineering*, Cancun, Mexico, 2008.
- [2] L. Montoya, "Geo-data acquisition through mobile GIS and digital video: an urban disaster management perspective," *Environmental Modeling & Software*, vol. 18, no. 10, pp. 869–876, 2003.
- [3] E. Lue, J. P. Wilson, and A. Curtis, "Conducting disaster damage assessments with spatial video, experts, and citizens," *Applied Geography*, vol. 52, pp. 46–54, 2014.
- [4] G. Yuan, S. Xia, and L. Zhang, "Trajectory outlier detection algorithm based on structural features," *The Journal of Computer Information Systems*, vol. 7, no. 11, pp. 4137–4144, 2011.
- [5] Y. Djenouri, D. Djenouri, and J. C. W. Lin, "Trajectory outlier detection," *ACM Transactions on Knowledge Discovery from Data*, vol. 15, no. 2, pp. 1–28, 2021.
- [6] A. Belhadi, Y. Djenouri, J. C. W. Lin, and A. Cano, "Trajectory outlier detection," *ACM Transactions on Management Information Systems*, vol. 11, no. 3, pp. 1–29, 2020.
- [7] M. Li, Z. Ma, and Y. Shan, "Traffic object's abnormal behavior recognition based on trajectory analysis," *Video Engineering*, vol. 36, no. 1, pp. 106–112, 2012.
- [8] J. Shi, Z. Pan, J. Fang, and P. Chao, "RUTOD: real-time urban traffic outlier detection on streaming trajectory," *Neural Computing and Applications*, vol. 1, p. 13, 2021.
- [9] J. Chi, C. Wu, and Y. Zhang, "Early fire disaster features research and detection method design in video images," in *2011 Symposium on Photonics and Optoelectronics (SOPO)*, Wuhan, China, 2011.
- [10] J. W. Mills, A. Curtis, and W. Fagan, *The Spatial Video Acquisition System as an Approach to Capturing Damage and Recovery Data after a Disaster: a Case Study from the Super Tuesday Tornadoes*, Natural Hazards Center, 2008.
- [11] B. Krausz and C. Bauckhage, "Loveparade 2010: automatic video analysis of a crowd disaster," *Computer Vision and Image Understanding*, vol. 116, no. 3, pp. 307–319, 2012.
- [12] T. Gupta, V. Nunavath, and S. Roy, "CrowdVAS-Net: a deep-CNN based framework to detect abnormal crowd-motion behavior in videos for predicting crowd disaster," in *2019 IEEE International Conference on Systems, Man and Cybernetics (SMC)*, Bari, Italy, 2019.
- [13] A. J. Thangam, P. T. Siva, and B. Yogameena, "Crowd count in low resolution surveillance video using head detector and color based segmentation for disaster management," in *2015 International Conference on Communications and Signal Processing (ICCSP)*, Melmaruvathur, India, 2015.
- [14] J. Wu and G. Zhou, "Real-time UAV video processing for quick-response to natural disaster," in *2006 IEEE International Symposium on Geoscience and Remote Sensing*, Denver, CO, USA, 2006.
- [15] N. Kerle, R. Stekelenburg, F. van den Heuvel et al., "Near-real time post-disaster damage assessment with airborne oblique video data," in *Geo-Information for Disaster Management*, P. Oosterom, S. Zlatanova, and E. M. Fendel, Eds., pp. 337–353, Springer, Berlin, Heidelberg, 2005.
- [16] D. Asahizawa, Y. Sato, and G. Sato, "Disaster surveillance video transmission system by wireless ballooned network," in *2009 International Conference on Advanced Information Networking and Applications Workshops*, Bradford, UK, 2009.
- [17] J. Zhou, S. Yi, J. Yang, L. Zhou, and L. Lu, "Disaster transmission network based on next-generation video standard," in *2019 International Conference on Intelligent Computing, Automation and Systems (ICICAS)*, Chongqing, China, 2019.
- [18] K. B. Kim, G. M. Geum, and C. B. Jang, "Research on the convergence of CCTV video information with disaster recognition and real-time crisis response system," *Journal of the Korea Convergence Society*, vol. 8, no. 3, pp. 15–22, 2017.
- [19] Z. Antoniou, A. S. Panayides, and M. S. Pattichis, "Adaptive emergency scenery video communications using HEVC for responsive decision support in disaster incidents," in *2015 37th Annual International Conference of the IEEE Engineering in Medicine and Biology Society (EMBC)*, Milan, Italy, 2015.
- [20] D. Chemodanov, P. Callyam, and K. Palaniappan, "Fog computing to enable geospatial video analytics for disaster-incident situational awareness," *Fog Computing: Theory and Practice*, pp. 473–503, 2020.
- [21] H. Tian and S. C. Chen, "A video-aided semantic analytics system for disaster information integration," in *2017 IEEE Third International Conference on Multimedia Big Data (BigMM)*, Laguna Hills, CA, USA, 2017.
- [22] H. Tian, H. C. Zheng, and S. C. Chen, "Sequential deep learning for disaster-related video classification," in *2018 IEEE Conference on Multimedia Information Processing and Retrieval (MIPR)*, Miami, FL, USA, 2018.
- [23] E. Charou, K. Kabassi, A. Martinis, and M. Stefouli, "Integrating multimedia GIS technologies in a recommendation system for geotourism," in *Multimedia Services in Intelligent Environments*, G. A. Tsihrintzis and L. C. Jain, Eds., vol. 3 of Smart Innovation, Systems and Technologies, pp. 63–74, Springer, Berlin, Heidelberg, 2010.
- [24] G. J. McDermid, S. E. Franklin, and E. F. LeDrew, "Remote sensing for large-area habitat mapping," *Progress in Physical Geography*, vol. 29, no. 4, pp. 449–474, 2005.
- [25] T. Navarrete and J. Blat, "VideoGIS: segmenting and indexing video based on geographic information," in *5th AGILE Conference on Geographic Information Science*, p. 9, Palma de Mallorca, Spain, 2002.
- [26] Z. Han, Y. Kong, and Q. Qin, "Geographic stereo video data analysis and model design," *Geography & Geo-Information Science*, vol. 29, no. 1, pp. 1–7, 2013.
- [27] J. Feng and H. Song, "Analysis of geographic video motion elements using random graph syntax," *Geomatics and Information Science of Wuhan University*, vol. 2, pp. 206–209, 2014.
- [28] A. Milosavljević, D. Rančić, A. Dimitrijević, B. Predić, and V. Mihajlović, "A method for estimating surveillance video georeferences," *ISPRS International Journal of Geo-Information*, vol. 6, no. 7, p. 211, 2017.
- [29] P. Lewis, S. Fotheringham, and A. Winstanley, "Spatial video and GIS," *International Journal of Geographical Information Science*, vol. 25, no. 5, pp. 697–716, 2011.
- [30] S. Walton, K. Berger, D. Ebert, and M. Chen, "Vehicle object retargeting from dynamic traffic videos for real-time visualisation," *The Visual Computer*, vol. 30, no. 5, pp. 493–505, 2014.
- [31] R. Du, S. Bista, and A. Varshney, "Video fields: fusing multiple surveillance videos into a dynamic virtual environment," in *Proceedings of the 21st International Conference on Web3D Technology*, California, July 2016.
- [32] C. Wu, Q. Zhu, Y. T. Zhang et al., "An adaptive organization method of geovideo data for spatiotemporal association

- analysis," *ISPRS Annals of the Photogrammetry, Remote Sensing and Spatial Information Sciences*, vol. 2, no. 4, p. 29, 2015.
- [33] Y. J. Cho, J. H. Park, and S. A. Kim, "Unified framework for automated person re-identification and camera network topology inference in camera networks," in *2017 IEEE International Conference on Computer Vision Workshops (ICCVW)*, Venice, Italy, 2017.
 - [34] H. Jian, J. Liao, X. Fan, and Z. Xue, "Augmented virtual environment: fusion of real-time video and 3D models in the digital earth system," *International Journal of Digital Earth*, vol. 10, no. 12, pp. 1177–1196, 2017.
 - [35] C. C. Loy, T. Xiang, and S. Gong, "Time-delayed correlation analysis for multi-camera activity understanding," *International Journal of Computer Vision*, vol. 90, no. 1, pp. 106–129, 2010.
 - [36] F. Mehboob, M. Abbas, S. Rehman, S. A. Khan, R. Jiang, and A. Bouridane, "Glyph-based video visualization on Google Map for surveillance in smart cities," *EURASIP Journal on Image and Video Processing*, vol. 2017, no. 1, 2017.
 - [37] X. Cai, B. Aydin, A. Ji, and R. Angryk, "A framework for local outlier detection from spatio-temporal trajectory datasets," in *2020 25th International Conference on Pattern Recognition (ICPR)*, Milan, Italy, 2020.
 - [38] X. Li, J. Han, and S. Kim, "ROAM: rule-and motif-based anomaly detection in massive moving object data sets," in *Proceedings of the 2007 SIAM International Conference on Data Mining*, 2007.
 - [39] W. Yang, Y. Gao, and L. Cao, "TRASMIL: a local anomaly detection framework based on trajectory segmentation and multi-instance learning," *Computer Vision and Image Understanding*, vol. 117, no. 10, pp. 1273–1286, 2013.
 - [40] P. R. Lei, "A framework for anomaly detection in maritime trajectory behavior," *Knowledge and Information Systems*, vol. 47, no. 1, pp. 189–214, 2016.
 - [41] S. Liu, L. M. Ni, and R. Krishnan, "Fraud detection from taxis' driving behaviors," *IEEE Transactions on Vehicular Technology*, vol. 63, no. 1, pp. 464–472, 2014.
 - [42] E. M. Knorr, R. T. Ng, and V. Tucakov, "Distance-based outliers: algorithms and applications," *The VLDB Journal*, vol. 8, no. 3-4, pp. 237–253, 2000.
 - [43] Y. Yu, L. Cao, E. A. Rundensteiner, and Q. Wang, "Outlier detection over massive-scale trajectory streams," *ACM Transactions on Database Systems*, vol. 42, no. 2, pp. 1–33, 2017.
 - [44] W. Chu, H. Xue, C. Yao, and D. Cai, "Sparse coding guided spatiotemporal feature learning for abnormal event detection in large videos," *IEEE Transactions on Multimedia*, vol. 21, no. 1, pp. 246–255, 2019.
 - [45] Q. Fu, J. Zhu, and Y. Chen, "An automatic learning model for trajectory outlier detection," in *Proceedings of the 3rd International Conference on Data Science and Information Technology*, 2020.
 - [46] E. Ristani, F. Solera, R. Zou, R. Cucchiara, C. Tomasi, and R. Zou, "Performance measures and a data set for multi-target, multi-camera tracking," in *Computer Vision – ECCV 2016 Workshops. ECCV 2016*, vol. 9914 of Lecture Notes in Computer Science, Springer, Cham.
 - [47] K. Kim, S. Oh, J. Lee, and I. Essa, "Augmenting aerial earth maps with dynamic information from videos," *Virtual Reality*, vol. 15, no. 2-3, pp. 185–200, 2011.
 - [48] N. Jiang, S. C. Bai, Y. Xu, C. Xing, Z. Zhou, and W. Wu, "Online inter-camera trajectory association exploiting person re-identification and camera topology," in *Proceedings of the 26th ACM International Conference on Multimedia*, 2018.
 - [49] F. T. Liu, K. M. Ting, and Z. H. Zhou, "Isolation forest," in *2008 Eighth IEEE International Conference on Data Mining*, Pisa, Italy, 2008.
 - [50] N. Shao, Y. Z. Zhou, and W. T. Hui, "Test data generation based on binary tree search space reduction," *Application Research of Computers*, vol. 31, no. 1, pp. 188–191, 2014.
 - [51] K. He, G. Gkioxari, and P. Dollár, "Mask R-CNN," in *Proceedings of the IEEE International Conference on Computer Vision*, Venice, Italy, October 2017.
 - [52] Y. Li, H. Li, X. Qian, and Y. Zhu, "A review and analysis of outlier detection algorithms," *Computer Engineering*, vol. 28, pp. 5–6, 2002.
 - [53] A. Lukežić, T. Vojir, L. C. Zajíč, J. Matas, and M. Kristan, "Discriminative correlation filter with channel and spatial reliability," in *2017 IEEE Conference on Computer Vision and Pattern Recognition (CVPR)*, Honolulu, HI, USA, 2017.
 - [54] Z. Zheng, L. Zheng, and Y. Yang, "Unlabeled samples generated by GAN improve the person re-identification baseline in vitro," in *2017 IEEE International Conference on Computer Vision (ICCV)*, Venice, Italy, 2017.
 - [55] C. Chen, D. Zhang, P. S. Castro et al., "iBOAT: isolation-based online anomalous trajectory detection," *IEEE Transactions on Intelligent Transportation Systems*, vol. 14, no. 2, pp. 806–818, 2013.
 - [56] M. Yetisgen-Yildiz and W. Pratt, "The effect of feature representation on MEDLINE document classification," in *AMIA Annual Symposium Proceedings*, San Francisco, November 2015.
 - [57] J. Mao, T. Wang, and C. Jin, "Feature grouping-based outlier detection upon streaming trajectories," *IEEE Transactions on Knowledge and Data Engineering*, vol. 29, no. 12, pp. 2696–2709, 2017.
 - [58] A. P. Bradley, "The use of the area under the ROC curve in the evaluation of machine learning algorithms," *Pattern Recognition*, vol. 30, no. 7, pp. 1145–1159, 1997.